International Journal of Machine Tools & Manufacture 50 (2010) 998–1005

Contents lists available at ScienceDirect

International Journal of Machine Tools & Manufacture

journal homepage: www.elsevier.com/locate/ijmactool

Tool point dynamics prediction by a three-component model utilizing distributed joint interfaces

Hamid Ahmadian *, Mostafa Nourmohammadi

Center of Excellence in Experimental Solid Mechanics and Dynamics, Iran University of Science and Technology, Narmak, Tehran 16846, Iran

ARTICLE INFO

Article history:
Received 4 February 2010
Received in revised form
12 July 2010
Accepted 14 July 2010
Available online 18 July 2010

Keywords:
Chatter vibration
Machine tool dynamics
Joint interface
Substructuring

ABSTRACT

In machine dynamics the tool point frequency response functions (FRFs) are employed to predict the stable machining conditions. In this paper, a combined analytical–experimental substructuring procedure is proposed to determine the tool point FRFs for different holder–tool configurations. The method employs the measured spindle-machine FRFs and analytical models of the tool and the holder to predict the tool tip FRFs for different sets of tools and holders mounted on the machine spindle without the need for repeated experimental measurements. Distributed joint interfaces are used to couple the three-component model of the machine. The machine tool tip FRFs with different tool–holder combinations are obtained assuming the clamping conditions at joint interfaces remain unchanged. An experimental case study is provided to demonstrate the applicability of the proposed method in dynamic modeling of machine tool.

1. Introduction

Chatter has long been a problem in machining operations. With trends for higher precision and reduced tolerances, solutions to avoid chatter in machining have become increasingly important. A common tool to identify chatter free machining conditions is the stability lobe diagram. A stability lobe diagram is a plot that separates unstable combinations of axial depth of cut, and spindle speed from the stable ones. Many studies have been performed and several criteria have been developed to generate stability lobe diagrams [1]. Knowledge of machine tool frequency responses is a prim need in many developed criteria for determining stable cutting conditions.

The tool tip frequency responses are obtained using experimental measurements and are changed with individual combinations of spindle, holder and tool configurations. Thus, there is a demand for semi-analytical methods that can predict machine tool dynamics using the minimum experimental measurements. This has been the subject of considerable research in the past. The simplest model for the machine tool treats the holder as a rigid base that supports a flexible tool [2–5]. But for non-slender tools, the dynamics of the spindle–holder has considerable effect on the tool point response. Schmitz et al. [6,7] divided the machine tool assembly into two separate substructures: overhang portion of the tool that is modeled analytically and the rest of the assembly, namely spindle–holder that is modeled experimentally. They employed receptance coupling substructure analysis (RCSA) to couple the dynamics of these two substructures using a lumped joint interface model.

In many circumstances the only variable portion of a machine center is the overhang portion of the tool; treatment mentioned in [6] can eliminate the need for repeated experimental works in these cases. Other researchers continued to improve this method and attempted to remove its drawbacks such as the need to measure rotational degrees of freedom (RDOF) at the joint interface [8–10]. In a recent work, Ahmadi and Ahmadian [11] modeled the tool dynamics considering the tool inserted shank resting on a resilient support. The support, provided by the spindle–holder, was represented by a damped-elastic foundation capable of simulating the dominant translational and rotational deformations of spindle over a wide frequency range. The support receptance functions, measured using a set of mobility experiments on spindle–holder assembly, were directly employed in the analytical model to represent the support dynamic properties. They modeled the joint interface between the tool and holder using an elastic interface layer where the interface stiffness can be defined as a variable function along the tool inserted shank length. Introduction of this layer enables one to take into account the variation in contact stiffness due to tool changes, interface contact pressure distribution, etc.

Schmitz and Duncan [12] developed an improved three-component model of the machine tool to extend RCSA method for a wide variety of spindle–holder–tool combinations. They separated the spindle–machine substructure into two parts: 1) the spindle and holder taper and (2) the remaining of the

* Corresponding author. Tel.: +9821 77240198; fax: +9821 77240488.
E-mail addresses: ahmadian@iust.ac.ir (H. Ahmadian), mo_noormohammadi@mecheng.iust.ac.ir (M. Nourmohammadi).

0890-6955/$ - see front matter © 2010 Elsevier Ltd. All rights reserved.
doi:10.1016/j.ijmachtools.2010.07.003

holder that was modeled analytically. Since the taper portion of the holder does not change from holder-to-holder, this three component model can predict the dynamics of the assembly for new assembly of spindle–holder–tool. In this work a stepped beam is employed to model the tapered section of the holder. More recently Filiz et al. [13] proposed a new method that uses the Timoshenko beam theory to model the complete holder–tool, including the actual tapered geometry.

In this paper, a new three-component model is proposed that can predict the tool dynamics without requiring any experimental measurement on the tool and holder. The spindle-machine is modeled experimentally by using the response model obtained from impact testing. Then in order to find the dynamics of the complete assembly, analytical models of the holder and tool are coupled to the experimental model of the spindle-machine. A new substructuring method is developed that couples machine tool components throughout continuous elastic joint interfaces. The interface stiffness is assumed to be a complex valued function to include the joint interface damping effects. The interface stiffness can be defined as a variable function along the continuous layer joints. As the normal pressure between substructures is varying along the joints, this enables the analyst to introduce the contact stiffness in more detail and as a result, a more precise prediction of the dynamics of the assembly can be obtained.

The remaining of the paper categorized as follows. The details of the mathematical modeling of assembled machine are proposed in Section 2. In Section 3 each component is considered separately and its appropriate dynamic model is obtained. These component models are assembled using the proposed thin interface layers to predict the dynamics of a specific machine center in Section 4 and the results are compared with those of experimental measurements to validate the model. Section 5 provides some conclusions from the present research study.

2. Tool–holder on a complex impedance support

The aim is to predict the dynamics of tool by coupling experimental response model of the spindle-machine and analytical/finite element models of the tool and holder. This coupling process occurs along continuous joint interfaces between these components. In this section a new methodology is developed to accomplish the task of coupling the three components.

The problem of connecting a tool and/or the holder to a flexible support with complex impedance using a continuous interface is commonly encountered in the dynamic modeling of machine tools. Consider the system of Fig. 1, comprised of a beam with variable cross-sections partly resting on a *flexible* support via an elastic interface layer with non-uniform stiffness properties. The flexible support is provided by the spindle-machine, substructure *A*, and substructure *B* resembles the tool and/or the holder. A linear elastic behavior is assumed for the interface layer, which has sufficient accuracy for small deformations [15]. The system has non-uniform properties, i.e. the beam and the elastic interface layer have varying geometric and stiffness properties, and thus in general no closed-form solution can be found for the problem.

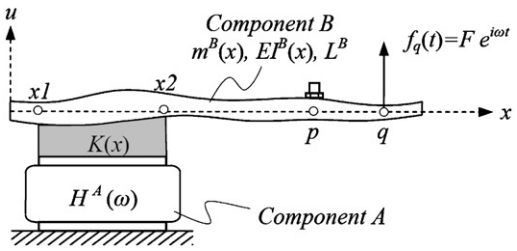

Fig. 1. A non-uniform beam coupled to a flexible support using an elastic layer interface.

In contrast to the substructure *A*, component *B* is a simpler one and its geometry and material properties are available with sufficient accuracy and its dynamic model can be obtained analytically. The modal model of substructure *B* is defined as followings:

$$[\Lambda^B]=\begin{bmatrix}\lambda_1^B & & 0\\ & \lambda_2^B & \\ 0 & & \lambda_n^B\end{bmatrix},\quad \{\phi^B(x)\}=\begin{Bmatrix}\phi_1^B(x)\\ \phi_2^B(x)\\ \vdots\\ \phi_n^B(x)\end{Bmatrix}, \tag{1}$$

where $\lambda_i^B,\phi_i^B(x)$, $i=1, 2, \ldots, n$ are squared natural frequencies and mode shapes of component *B*. The number of modes that are considered in the modal model, *n*, depends on the frequency range of interest and the desired degree of model accuracy. Note that the modal model of component *B* is represented in unassembled state, i.e. it contains the rigid body modes. The mode shapes are mass normalized and satisfy the following orthogonality conditions:

$$\int_0^{L^B} m^B(x)\phi_i^B(x)\phi_j^B(x)dx=\delta_{ij},$$
$$\int_0^{L^B} \phi_i^B(x)\frac{d^2}{dx^2}\left[EI^B(x)\frac{d^2}{dx^2}\phi_j^B(x)\right]dx=\lambda_i^B\delta_{ij}, \tag{2}$$

where $m^B(x)$ and $EI^B(x)$ are linear mass density and flexural stiffness of component *B*.

On the other hand, the complex substructure *A* is comprised of many parts and internal joints, and there is no enough information about dynamic behavior of these parts to build a reliable model to prediction its dynamic response. In this study substructure *A* is regarded as a black box with known input–output relations at few DOFs obtained from experimental measurements. Such decomposition seems logical in modeling machine tool dynamics. The tool and holder are geometrically simple components and their properties are available. In contrast the rest of the machine tool, namely spindle-machine substructure (all the parts and joints that exist between the holder and ground such as bearings, casings, gear train and spindle) consists of many parts and internal unknown joints. Thus, it is reasonable to model the tool and/or holder analytically and then couple them to the experimental model of spindle-machine substructure in order to predict the dynamics of the whole structure.

In order to find the response of the system, each component is considered separately and the adjacent structure contribution is represented as distributed forces. In presence of harmonic excitation at the tool tip the interface distributed forces are also harmonic and proportional to the difference between the displacements of the two components:

$$F^A(x)=K(x)[U^B(x)-U^A(x)],$$
$$F^B(x)=-F^A(x). \tag{3}$$

Here $U^A(x)$ and $U^B(x)$ are the deformed shapes of the components *A* and *B* in frequency domain and $K(x)$ is the interface stiffness function. The deformed shapes are complex functions due to non-proportional nature of damping in the spindle-machine substructure and $F^A(x)$, and $F^B(x)$ are complex valued distributed forces exerted on each component along the joint interface.

Deformations of the components can be determined if the distributed forces acting on the components along the interface

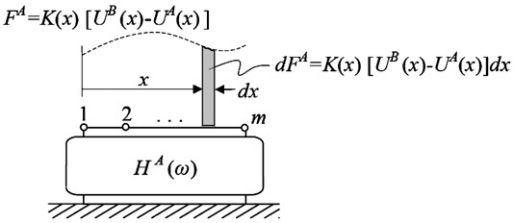

Fig. 2. Differential force at the joint interface acting on the component *A*.

are identified. First we consider the measured receptance matrix $[H^A(\omega)]$, i.e. the input–output relations of substructure *A* at selected points ($i=1, 2, \ldots, m$) located within the interface

$$[H^A(\omega)]=\begin{bmatrix} H^A_{11} & H^A_{12} & \cdots & H^A_{1,m} \\ H^A_{21} & H^A_{22} & \cdots & H^A_{2,m} \\ \vdots & \vdots & \ddots & \vdots \\ H^A_{m,1} & H^A_{m,2} & \cdots & H^A_{m,m} \end{bmatrix} \tag{4}$$

The transfer functions of the substructure *A* are measured at discrete points along the joint interface by impact testing. Fig. 2 shows these discrete points. The analysis of interface forces specified in Eq. (3) requires the force–displacement relations at all interface points. We define a *continuous* receptance function $H^A_{i,x}$ at any point along the joint interface (the deflection of component *A* along the interface as a function of *x* due to the unit harmonic excitation at point *i*) by curve fitting the measured receptances. The system under consideration is linear within the excitation load and frequency range of interest, and $H_{i,x}=H_{x,i}$. The continuous receptance function can be approximated using a power series as

$$H^A_{i,x}\cong\sum_{j=1}^{m}\alpha_{ij}x^{j-1}=\begin{bmatrix}\alpha_{i1} & \alpha_{i2} & \cdots & \alpha_{i,m}\end{bmatrix}\{x\},\quad i=1, 2, \ldots, m, \tag{5}$$

or in matrix form as

$$\{H^A_x\}=\begin{Bmatrix} H^A_{1,x} \\ H^A_{2,x} \\ \vdots \\ H^A_{m,x} \end{Bmatrix}=\begin{bmatrix} \alpha_{11} & \alpha_{12} & \cdots & \alpha_{1,m} \\ \alpha_{21} & \alpha_{22} & \cdots & \alpha_{2,m} \\ \vdots & \vdots & \ddots & \vdots \\ \alpha_{m,1} & \alpha_{m,2} & \cdots & \alpha_{m,m} \end{bmatrix}\begin{Bmatrix} 1 \\ x \\ \vdots \\ x^{m-1} \end{Bmatrix}=[\alpha]\{x\}, \tag{6}$$

where the vector $\{x\}=[1\ x\ \ldots\ x^{m-1}]^{\mathrm{T}}$. Evaluating Eq. (6) at discrete measurement points x_i leads to

$$\begin{bmatrix} H^A_{11} & H^A_{12} & \cdots & H^A_{1,m} \\ H^A_{21} & H^A_{22} & \cdots & H^A_{2,m} \\ \vdots & \vdots & \ddots & \vdots \\ H^A_{m,1} & H^A_{m,2} & \cdots & H^A_{m,m} \end{bmatrix}=\begin{bmatrix} \alpha_{11} & \alpha_{12} & \cdots & \alpha_{1,m} \\ \alpha_{21} & \alpha_{22} & \cdots & \alpha_{2,m} \\ \vdots & \vdots & \ddots & \vdots \\ \alpha_{m,1} & \alpha_{m,2} & \cdots & \alpha_{m,m} \end{bmatrix}$$
$$\begin{bmatrix}\{X_1\} & \{X_2\} & \cdots & \{X_m\}\end{bmatrix} \tag{7}$$

The vector $\{X_i\}$ equals the vector $\{x\}$ evaluated at *i*th point. The matrix $[\alpha]$ is obtained as

$$[\alpha(\omega)]=\left[H^A(\omega)\right][X^A]^{-1},\quad \left[X^A\right]=\begin{bmatrix}\{X_1\} & \{X_2\} & \cdots & \{X_m\}\end{bmatrix}, \tag{8}$$

and as a result the receptance function $H^A_{i,x}$ is known. Next, we turn our attention to the force–displacement relations in the joint interface. Fig. 2 shows the differential force acting on the component *A* at the joint interface. Deflection of point *i* as a result of this differential force can be expressed as

$$dU^A_i=H^A_{i,\,x}dF^A=H^A_{i,\,x}K(x)[U^B(x)-U^A(x)]dx. \tag{9}$$

One may employ the superposition of the effects of all forces acting on substructure *A* in order to determine the deformation in point *i*, i.e.

$$U^A_i=\int_{x1}^{x2}H^A_{i,\,x}K(x)[U^B(x)-U^A(x)]dx,\quad i=1, 2, \ldots, m \tag{10}$$

The unknown deflection shapes $U^A(x)$ and $U^B(x)$ are approximated with the following series expressions:

$$U^A(x)\cong\sum_{j=1}^{m}a_jx^{j-1}=\{x\}^T\{a\}, \tag{11}$$

$$U^B(x)\cong\sum_{j=1}^{n}b_j\phi^B_j(x)=\{\phi^B\}^T\{b\} \tag{12}$$

The displacement field of component *A* along the interface is approximated by a polynomial of order $m-1$, consistent with the earlier assumption used in Eq. (5). On the other hand, the mode shapes of the component *B*, i.e. $\phi^B_j(x)$ are available. Thus, employing the expansion theorem, its displacement field at the interface is approximated by the finite sum of its mode. Introducing expansions defined in Eqs. (11) and (12) in Eq. (10), one obtains

$$\{X_i\}^T\{a\}=\int_{x1}^{x2}H^A_{i,\,x}K(x)[\{\phi^B\}^T\{b\}-\{x\}^T\{a\}]dx,\quad i=1, 2, \ldots, m, \tag{13}$$

which in matrix form can be defined as

$$[X^A]^T\{a\}=\int_{x1}^{x2}K(x)\{H^A_x\}[\{\phi^B\}^T\{b\}-\{x\}^T\{a\}]dx \tag{14}$$

Eq. (13) includes a frequency dependent integral that can be simplified using the expression given in Eq. (6). Introducing Eqs. (6) and (8) in Eq. (14) the governing equation of the component *A* can be obtained as follows:

$$\left([X^A]^T+[H^A][X^A]^{-1}\int_{x1}^{x2}K(x)\{x\}\{x\}^T\,dx\right)\{a\}$$
$$-\left([H^A][X^A]^{-1}\int_{x1}^{x2}K(x)\{x\}\{\phi^B\}^T\,dx\right)\{b\}=\{0\} \tag{15}$$

Eq. (15) has an important computational advantage that is its integrals are frequency independent and there is no need to evaluate the integrals at each individual frequency of interest. Eq. (15) consists of *m* equations with $m+n$ unknowns therefore *n* complementary equations are required to solve these equations. In the followings these complementary equations are obtained from the governing equations of the substructure *B*.

Substructure *B* is modeled as an Euler–Bernoulli beam theory. Later in the next section it is shown that this simple model is adequate for modeling machine tool within the frequency range of interest in HSM. However, more detailed models taking into account shear deformation and rotational inertia are required when the system behavior at higher frequencies is considered. Equation of motion of substructure *B* is

$$m^B(x)\frac{\partial^2u^B(x,t)}{\partial t^2}+\frac{\partial^2}{\partial x^2}\left[EI^B(x)\frac{\partial^2u^B(x,t)}{\partial x^2}\right]=p^B(x,t) \tag{16}$$

where $p^B(x,t)$ is the distributed lateral load. Referring to Fig. 1 the distributed load $p^B(x,t)$ is divided into two terms: a concentrated force at point *q* and a distributed load acting on substructure *B* from the elastic interface layer:

$$p^B(x,t)=\delta(x-x_q)f_q(t)+K(x)[u^A(x,t)-u^B(x,t)], \tag{17}$$

in which $\delta(x-x_q)$ is the unit impulse function and $K(x)$ is a known function within the joint interface domain. As shown in Fig. 1, a harmonic force $f_q(t)=Fe^{i\omega t}$ is applied at point *q*. The system experiences a harmonic motion in both substructures and using

Eqs. (11) and (12) these motions are expressed as

$$u^A(x,t) = U^A(x)e^{i\omega t} \cong \left(\sum_{j=1}^{m} a_j x^{j-1}\right) e^{i\omega t}, \tag{18}$$

$$u^B(x,t) = U^B(x)e^{i\omega t} \cong \left(\sum_{j=1}^{n} b_j \phi_j^B(x)\right) e^{i\omega t} \tag{19}$$

Note that when the damping mechanism of the system is non-proportional, the motions are not synchronous and functions $U^A(x)$ and $U^B(x)$ are complex. Inserting the expressions developed for harmonic motion of the substructures into equation of motion of substructure B, expressed in Eq. (16), one obtains

$$-\omega^2 m^B(x)\sum_{j=1}^{n} b_j\phi_j^B(x) + \frac{d^2}{dx^2}\left(EI^B(x)\sum_{j=1}^{n} b_j \frac{d^2}{dx^2}\phi_j^B(x)\right) = \delta(x-x_q)F + K(x)\left(\sum_{j=1}^{m} a_j x^{j-1} - \sum_{j=1}^{n} b_j\phi_j^B(x)\right) \tag{20}$$

Projecting the equation of harmonic motion (20) on the Eigenfunctions $\phi_i^B(x)$ produces n more equations in terms of unknown coefficients a_i and b_i as

$$-\omega^2 b_i + \lambda_i^B b_i = \int_{x1}^{x2} \phi_i^B(x)K(x)\left(\sum_{j=1}^{m} a_j x^{j-1} - \sum_{j=1}^{n} b_j\phi_j^B(x)\right)dx + F\phi_i^B(x_q), \quad i = 1, 2, \ldots, n \tag{21}$$

Eq. (21) can be rearranged in matrix from as

$$\left(-\int_{x1}^{x2} K(x)\{\phi^B\}\{x\}^T dx\right)\{a\} + \left([\Lambda^B] - \omega^2[I] + \int_{x1}^{x2} K(x)\{\phi^B\}\{\phi^B\}^T dx\right)\{b\} = F\{\phi^B(x_q)\} \tag{22}$$

Simultaneous solution of Eqs. (15) and (22) leads to unknown vectors $\{a\}$ and $\{b\}$. Note that the coefficients of Eqs. (15) and (22) contain the measured receptance matrix $[H^A]$ and the term $\omega^2[I]$. Hence, vectors $\{a\}$ and $\{b\}$ are frequency dependent and must be determined in each individual frequency of interest.

The steady-state response of the system to harmonic force $f_q(t)$ can be found using known vectors $\{a\}$ and $\{b\}$. Evaluating the deflection shapes at any desired point, produces the transfer function between that point and the point of excitation, e.g. the frequency response function at point p due to excitation at point q (shown in Fig. 1):

$$H_{pq}(\omega) = \frac{U^B(x_p)}{F} = \sum_{j=1}^{n} b_j(\omega)\phi_j^B(x_p) \tag{23}$$

The method proposed in this section is a substructuring technique with added capabilities. The conventional coupling methods join the substructures at discrete points, while the proposed method couples substructures along a distributed joint interface. Moreover, it is a multi-domain method that couples a substructure with known model in frequency domain to another model in modal domain, a very useful capability in modeling machine tool dynamics.

The proposed substructuring method can couple several substructures together. Consider a system comprised of three substructures, as shown in Fig. 3a, connected using two different distributed interfaces. The substructures A, B and C represent the spindle-machine, holder and tool, respectively. The information available about substructure A is its FRFs measured at finite points while analytical models of substructures B and C are available.

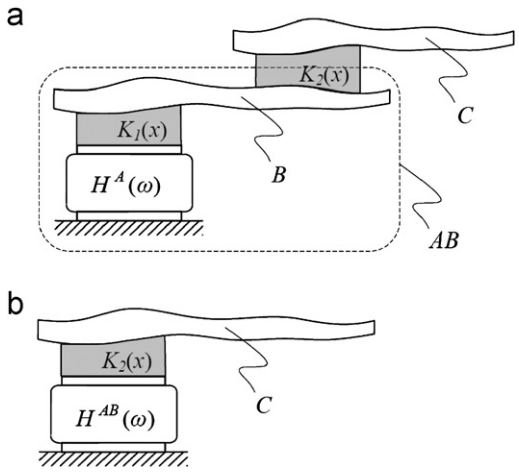

Fig. 3. A system comprises of three substructures (a). Substructures A and B coupled together and form a new substructure AB (b).

Coupling of these three substructures is performed in two steps. First, substructures A and B are coupled together through an elastic layer interface to create a new substructure AB as indicated in Fig. 3b. Then in the second step, by coupling the substructures AB and C, the dynamics of the whole assembly is obtained. The following demonstrated the process of coupling a spindle-machine substructure to the holder and tool substructures using the proposed method.

3. Component dynamic models

In order to perform substructure coupling using the proposed method, appropriate models of all substructures are needed. The component models may be presented in the modal or frequency domains.

The available information regarding the spindle-machine substructure is usually incomplete experimental data in frequency domain. These data are in fact the FRFs that are extracted by experimental measurement at a few points of the substructure. The number of points that are chosen in measurement depends on the length of the joint interface, desired degree of accuracy and the restrictions that may exist in experimental measurement. Fig. 4 shows the three measurement points of a spindle taper that were selected to construct FRF matrix of this substructure, using impact testing. Instrumented impact hammer Brüel&Kjær 8202 was used to excite the spindle taper and responses were measured using a Brüel&Kjær 4393 accelerometer. Both measured input force and output responses were transformed from time domain to frequency domain using a dual channel spectrum analyzer Brüel&Kjær 2032 and their ratio, i.e. the frequency response is obtained. As indicated in Fig. 4 points 1 and 2 could not be excited by the hammer. Thus, some elements of the FRF matrix cannot be obtained directly from experimental measurements.

By exciting the spindle at point 3 and measuring the responses, one column of spindle-machine FRF matrix is measured, namely H_{13}^S, H_{23}^S and H_{33}^S. The plots of the measured FRFs are shown in Fig. 5. Inspecting these plots, it is evident that the damping is very high and extracting modal model from these data is impractical. This leads to employing a frequency domain model for the spindle-machine substructure. The method presented in this paper is developed based on the assumption that an accurate analytical/numerical model can be developed for the tool and the holder. But the rest of machine including its spindle cannot be

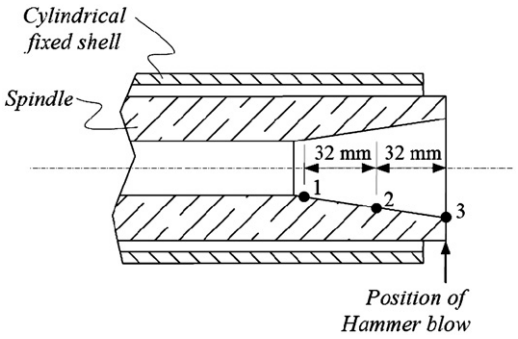

Fig. 4. Selected points of the spindle taper for impact testing.

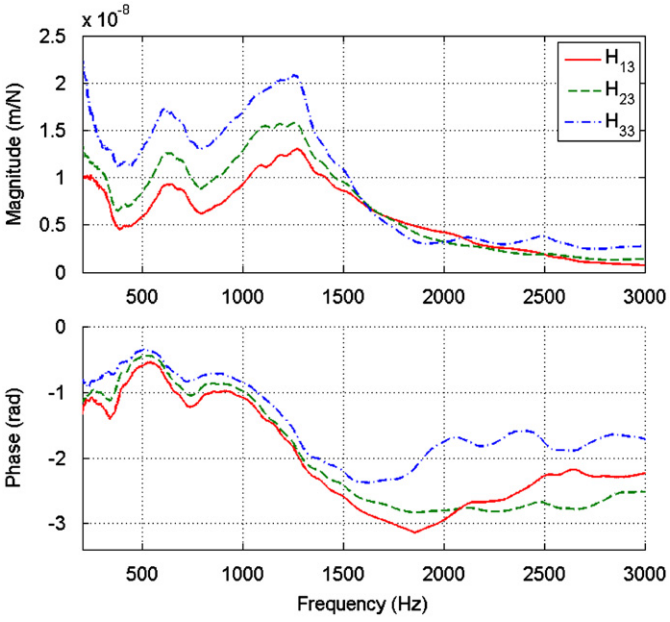

Fig. 5. Measured frequency responses of the spindle taper.

modeled accurately and hence the spindle measured data are directly employed to predict the dynamics of spindle/holder/tool assembly. The obtained machine tool model, a hybrid analytical–experimental model, is developed using minimum experimental data and is capable to predict the dynamics of machine assembly with different holder/tool combinations.

The remaining elements of the FRF matrix are obtained from the measured FRFs using the following relations:

$$H_{11}^S = \frac{U_1^S}{F_1} = \frac{U_1^S}{F_3}\frac{F_3}{U_3^S}\frac{U_3^S}{F_1} = \frac{(H_{13}^S)^2}{H_{33}^S}, \quad H_{22}^S = \frac{(H_{23}^S)^2}{H_{33}^S},$$
$$H_{12}^S = H_{21}^S = \frac{H_{13}^S H_{23}^S}{H_{33}^S} \tag{24}$$

Next we consider the holder substructure. A collet-type tool holder with steep taper shank is used in the experimental case studies. The tool holder is secured in spindle taper with a threaded drawbar and the tool is clamped to the tool holder using a tapered collet and a clamping nut. In order to couple this substructure to the spindle-machine, an analytical model of holder is developed and its modal model is used for the analysis. The steel holder used in this work is shown in Fig. 6 and its dimensions are given in Table 1.

The holder is modeled as a multi-stepped beam as shown in Fig. 6(b). It is a non-slender short component and one would think

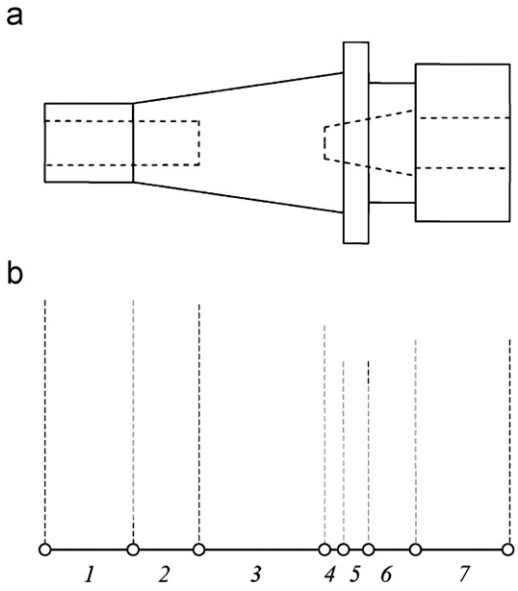

Fig. 6. The tool holder (a) and its equivalent multi-span beam model (b)

Table 1
Dimensional properties of the holder shown in Fig. 6.

Section (mm)	1	2	3	4	5	6	7
D_i	14	14	0	10–12	12-15	15–21	16
D_o	25	25–31	31–43	43–44	64	38	50
L	28	21	40	6	8	15	30

a Timoshenko beam model must be adopted to take into account shear deformation and rotary inertia effects of the beam. As discussed in Ref. [14] consideration of these effects does not improve the tool point FRF prediction significantly in lower modes. The frequency range of interest in high speed machining that features spindle speeds of 10,000–40,000 RPM covers the first few bending modes of tool and adopting the Euler–Bernoulli beam theory is adequate in this application.

The holder has tapered sections that can be modeled with stepped beam sections, i.e. each tapered section is replaced with one or more stepped beams and the mean diameters of the original tapered sections is chosen for the corresponding equivalent straight beams. Filiz et al. [13] showed that the error from the straight beam approximation is negligible if the diameter ratio of tapered segments are less than 2. This criterion is employed in modeling conical sections of the holder.

The remaining substructure of this assembly is the tool that is the simplest one from modeling point of view. In order to connect this substructure to the holder, its modal model is required. Since the tool is normally a slender part, an Euler–Bernoulli stepped beam model can precisely predict its dynamic behavior. In the present study, two different cylindrical blanks are used instead of the real fluted tools.

4. Coupling substructures using distributed joint interfaces

The first step in prediction of tool point FRF is coupling the holder substructure to the spindle and obtaining the dynamic model of the assembly in frequency domain. Fig. 7 shows the concept of coupling these substructures. The obtained holder–spindle assembly frequency response model is then coupled with the tool model to evaluate the dynamics of the whole structure

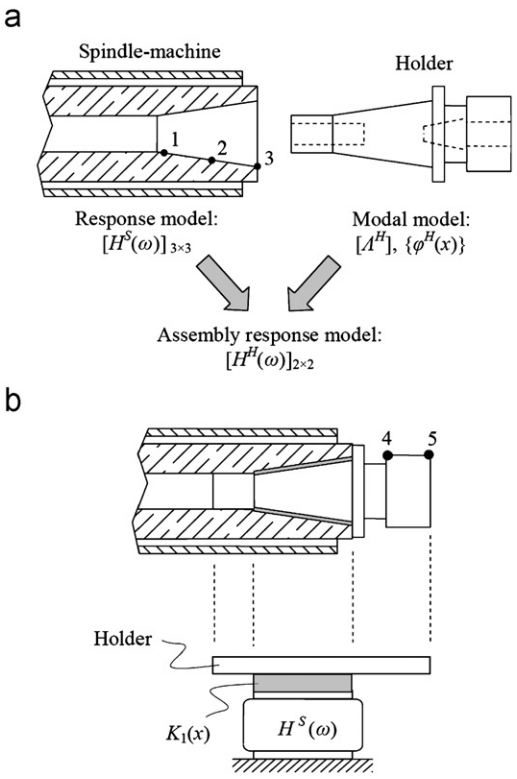

Fig. 7. The machine spindle and holder (a) and their assembled representative model (b)

particularly at the tool tip. The modal model of the holder is coupled to the response model of spindle-machine to produce the frequency responses of the assembly. The obtained response model comprises of direct and cross frequency response functions of the assembly at points 4 and 5, as shown in Fig. 7. As a first step the properties of joint interface between these substructures are identified. In this study, the experimentally measured FRF of the spindle–holder assembly at point 5 is used and the parameters of the joint interface are identified by minimizing the discrepancy between predicted and observed FRFs at this point.

Since the contact between the holder and spindle has a considerable length, variation in the interface stiffness is significant. Thus, by using uniform properties for the interface layer, an accurate prediction of the system dynamics may not be achieved. Namazi et al. [15] studied the variation in the stiffness of the joint interface between the spindle and holder. They modeled this interface layer using uniformly distributed translational and rotational springs at the contact zone. By experimental verification, they proposed a linear model for the stiffness of this layer as

$$K_1(x) = k_1\left(D_1 + \frac{D_2 - D_1}{L_{j1}}x\right), \tag{25}$$

where parameters D_1 and D_2 are the smaller and the larger diameters of the holder taper, respectively, L_{j1} is the length of the taper contact, and k_1 is the interface stiffness coefficient. In the present study, a structural damping model is adopted for the joint interface $k_1 = k(1+i\eta)$ as it is more descriptive of joint interfaces damping mechanism compared to the viscous damping model adopted in previous studies [16]. The parameter η in this definition is the interface structural damping coefficient. The corresponding parameters of the holder are tabulated in Table 1. An optimization exercise is conducted to obtain optimum values of the joint interface parameters, namely k and η while the objective function is defined as the deviation of the predicted FRF at the free end of the holder from the corresponding measured one. Table 2 shows the identified values for the holder–spindle joint interface obtained by minimizing this objective function and Fig. 8 compares the predicted and measured frequency response functions of the spindle–holder assembly at the holder free end.

The second step in modeling machine tool dynamics and determining the tool point FRF is coupling the tool model to the holder–spindle assembly. The idea is eliminating any repeated experimentation on the tool and holder, so that all measurements are limited to the previously measured spindle-machine FRFs. Moreover, by adding analytical model of any chosen tool and holder, the dynamics of the whole structure is obtained.

Table 3 tabulates the properties of the tools used in verifications of this study. Using a short tool causes the spindle and holder to have significant effect on the response at the tool point. Otherwise, if a long and very flexible tool is used, then the dynamics of the system is mainly affected by the tool and the errors in modeling other substructures and identification of joints would not be detectable. As shown in Fig. 7, the contact between the tool and holder occurs along a short length. Hence, responses at two points of the holder (points 4 and 5 as shown in Fig. 7) are used to construct the frequency response model of the spindle–holder assembly.

Table 2
The identified properties of the joint interface between the spindle and the holder.

k (N/m^2)	η
1.26×10^{12}	0.45

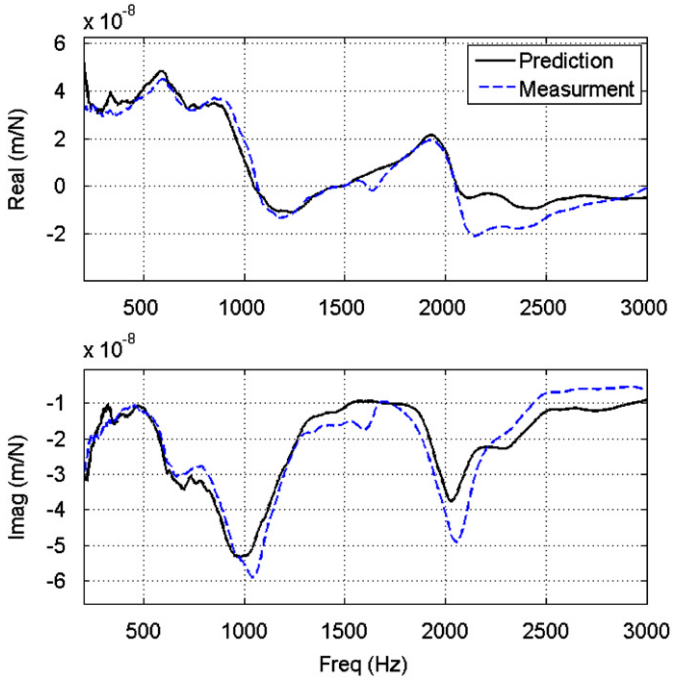

Fig. 8. The predicted and measured FRFs of spindle–holder at holder free end.

Table 3
The tool dimensions (mm).

	Total length	Shank length	Diameter
Short tool	100	30	16
Long tool	200	30	16

Ahmadi and Ahmadian [11] proposed a linear model for the variation of the stiffness in the second joint interface as

$$K_2(x) = (k_0 + k_1 x)(1 + i\zeta) \tag{26}$$

They verified by experiment that this first order model adequately describes the joint behavior and higher order models do not give considerable improvement in predictions. A similar optimization procedure is used to identify the parameters of this interface as previous one. Table 4 gives the optimum parameters of the second joint interface and Fig. 9 compares the predicted tool point FRF with the measured one.

In order to validate the capability of the proposed method of this paper in prediction of tool tip FRFs, the short tool is replaced with a long tool whose properties are given in Table 3. The long tool is mounted using the same clamping torques and contact lengths as used in the case of short tool to ensure the changes in the joint interfaces parameters are negligible. Fig. 10 compares the predicted tool point FRF with the measured one. As shown in this figure, the identified model predicts the behavior of the system with required accuracy in a different machine tool configuration.

Table 4
Identified properties of the joint interface between the holder and the tool.

k_0 (N/m^2)	k_1 (N/m^3)	ζ
7.32×10^{10}	-7.42×10^{11}	0.25

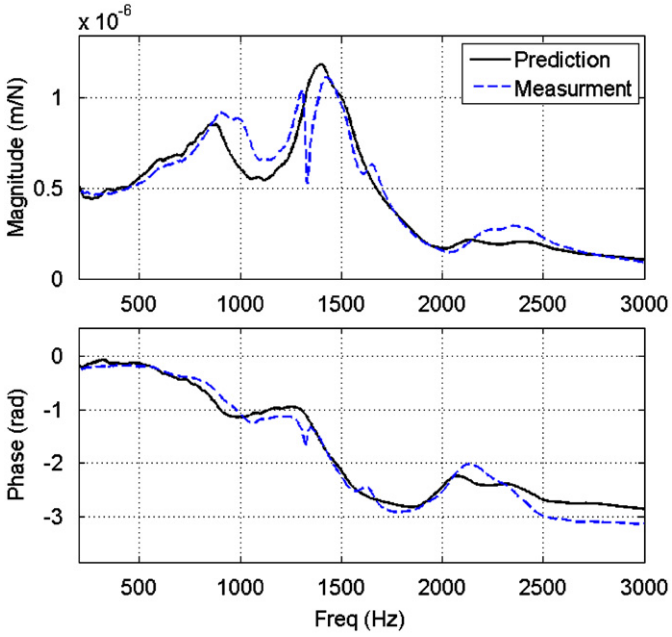

Fig. 9. The measured and predicted tool tip receptances using three component modeling of the end mill (short tool).

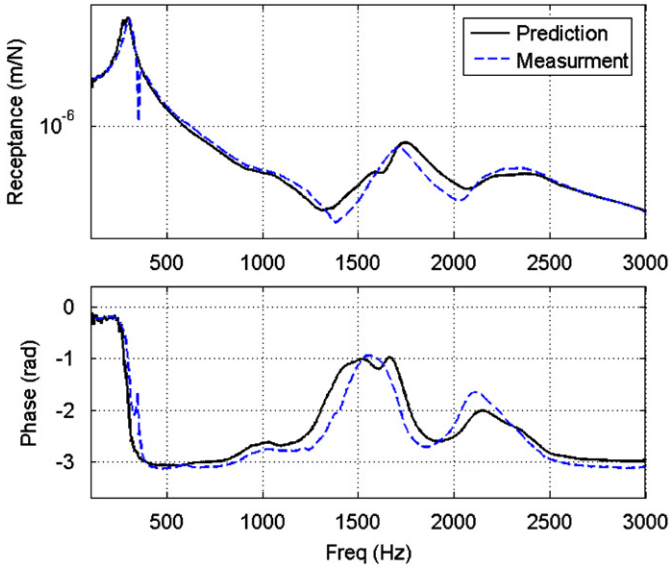

Fig. 10. Tool point FRFs using three component modeling of the end mill (long tool).

5. Conclusions

A new substructuring method is proposed capable of coupling the dynamics of different machine components through a continuous damped-elastic layer interface. This is the case in machine tool where the connections between components do not occur in a single point, but along a distributed joint interface. By using this new approach, a three-component model of the machine tool is developed. The model employs the measured dynamic flexibility of the spindle-machine assembly and analytic models of the holder and tool to predict the dynamic behavior of the whole assembly. Utilizing this model, the analyst can predict the machining dynamics in various combinations of tool and holder without the need for repeated measurements. The proposed distributed parameter joint interfaces take into account the change in stiffness along the joint interfaces, and also use a displacement dependent damping mechanism to account for structurally damped characteristics of the interfaces. The interface layer parameters are identified using an optimization procedure by minimizing the difference between predicted and measured dynamic behavior of the machine assembly. The conducted experimental study verifies the reliability of the proposed coupling method and its capability in predicting the structure dynamics.

References

[1] E. Budak, Y. Altintas, Analytical prediction of chatter stability in milling—Part I: general formulation; Part II: application to common milling systems, Transactions of ASME, Journal of Dynamic Systems, Measurement, and Control 120 (1998) 22–36.
[2] E.B. Kivanc, E. Budak, Structural modeling of end mills for form error and stability analysis, International Journal of Machine Tools and Manufacture 44 (11) (2004) 1151–1161.
[3] E. Budak, Analytical models for high performance milling. Part I: cutting forces, structural deformations and tolerance integrity, International Journal of Machine Tools and Manufacture 46 (12–13) (2006) 1478–1488.
[4] E. Budak, Analytical models for high performance milling. Part II: process dynamics and stability, International Journal of Machine Tools and Manufacture 46 (12–13) (2006) 1478–1488.
[5] H. Ahmadian, M. Salahshour, Continuous model for analytical prediction of chatter in milling, International Journal of Machine Tools and Manufacture 49 (2009) 1136–1143.
[6] T.L. Schmitz, Predicting high-speed machining dynamics by substructure analysis, Annals of the CIRP (2000) 303–308.
[7] T.L. Schmitz, M.A. Davies, M.D. Kennedy, Tool point frequency response prediction for high-speed machining by RCSA, Transactions of the ASME, Journal of Manufacturing Science and Engineering 123 (2001) 700–707.
[8] S.S. Park, Y. Altintas, M. Movahhedy, Receptance coupling for end mills, International Journal of Machine Tools and Manufacture 43 (2003) 889–896.
[9] M.R. Movahhedy, J.M. Gerami, Prediction of spindle dynamics in milling by sub-structure coupling, International Journal of Machine Tools and Manufacture 46 (2006) 243–251.

[10] G.S. Duncan, M.F. Tummond, T.L. Schmitz, An investigation of the dynamic absorber effect in high-speed machining, International Journal of Machine Tools and Manufacture 45 (2005) 497–507.
[11] K. Ahmadi, H. Ahmadian, Modelling machine tool dynamics using a distributed parameter tool–holder joint interface, International Journal of Machine Tools and Manufacture 47 (2007) 1916–1928.
[12] T. Schmitz, G.S. Duncan, Three-component receptance coupling substructure analysis for tool point dynamics prediction, ASME Journal of Manufacturing Science and Engineering 127 (2005) 781–790.
[13] S. Filiz, C.-H. Cheng, K.B. Powell, T.L. Schmitz, O.B. Ozdoganlar, An improved tool–holder model for RCSA tool–point frequency response prediction, International Journal of Precision Engineering 33 (2009) 26–36.
[14] A. Ertürk, Özgüven, E. Budak, Analytical modeling of spindle–tool dynamics on machine tools using Timoshenko beam model and receptance coupling for the prediction of tool point FRF, International Journal of Machine Tools and Manufacture 46 (2006) 1901–1912.
[15] M. Namazi, Y. Altintas, T. Abe, N. Rajapakse, Modeling and identification of tool holder–spindle interface dynamics, International Journal of Machine Tools and Manufacture 47 (2007) 1333–1341.
[16] A.A. Ferri, A.C. Bindemann, Damping and vibration of beams with various types of frictional support conditions, ASME Journal of Vibration and Acoustics 114 (1992) 289–296.